PNAS RESEARCH ARTICLE | MICROBIOLOGY OPEN ACCESS

Macropinosomes are a site of HIV-1 entry into primary CD4$^+$ T cells

Tomoyuki Murakami[a,1], Ricardo de Souza Cardoso[a], Praveen Manivannan[a], Ya-Ting Chang[a], Eric Rentchler[b], Kai-Neng Chou[a], Yipei Tang[a], Joel A. Swanson[a], Philip D. King[a,1], and Akira Ono[a,1]

Affiliations are included on p. 10.

Edited by John Coffin, Tufts University, Boston, MA; received August 29, 2024; accepted May 6, 2025

HIV-1 has been observed to enter target cells at both the plasma membrane and endosomes. However, which pathways mediate its entry into primary CD4$^+$ T cells, the major targets of this virus, remains unclear. Here, we show that HIV-1 can enter primary CD4$^+$ T cells through macropinocytosis, a form of endocytosis. We found that HIV-1 can enter primary CD4$^+$ T cells at both the plasma membrane and internal compartments, while entry into common T cell lines occurred primarily at the plasma membrane. Inhibition of macropinocytosis suppressed HIV-1 internalization into and subsequent fusion with primary CD4$^+$ T cells regardless of the viral coreceptor usage. Microscopic analysis of viral contents exposed to the cytosol confirmed that HIV-1 fusion occurs at the macropinosomal membrane. Finally, the inhibition of macropinocytosis blocked HIV-1 infection of primary CD4$^+$ T cells. Altogether, this study identifies macropinocytosis as one pathway for HIV-1 entry into primary CD4$^+$ T cells.

virus entry | macropinocytosis | virus-cell fusion | primary CD4$^+$ T cell | HIV-1

Significance

HIV-1 entry is an important therapeutic target. However, the exact subcellular location of HIV-1 entry into primary CD4$^+$ T cells, a major in vivo host for HIV-1, remains undetermined. The current study shows that macropinosomes serve as a site for productive HIV-1 entry into the cytoplasm of primary CD4$^+$ T cells. Supporting the role for macropinosomes, inhibition of macropinocytosis prevents HIV-1 internalization into, fusion with, and infection of primary CD4$^+$ T cells. By contrast, infection of a CD4$^+$ T cell line commonly used in HIV-1 research is insensitive to macropinocytosis inhibition. Altogether, this study highlights the primary T cell–specific dependence of HIV-1 on macropinocytosis and therefore suggests the macropinosome-mediated HIV-1 entry as a potential target for antiviral strategies.

The HIV-1 entry process consists of attachment of a virus particle to target cells and subsequent fusion of viral and target cell membranes. These processes are mediated by the interactions between the HIV-1 envelope glycoprotein (Env) and the receptor CD4 and coreceptors CCR5 or CXCR4 on target cells. While the molecular mechanisms that lead to fusion are well understood, the site of HIV-1 entry remains uncertain.

HIV-1 can fuse with target cells at neutral pH (1, 2), indicating that acidification of endosomal compartments is dispensable for HIV-1 entry. In addition, mutagenesis of the CD4 cytoplasmic tail, which impairs ligand-induced internalization, does not block HIV-1 infection (3, 4). These observations support the possibility that HIV-1 fusion takes place at the plasma membrane. However, using pharmacological or genetic inhibition of endocytosis and live cell imaging, other studies have indicated that HIV-1 enters cells through an endocytic route in a HeLa cell-derived cell line, TZM-bl, and a T cell line, CEM (5). Inhibition of endocytosis either with PitStop2, a clathrin-mediated endocytosis-specific inhibitor, or by expression of dominant negative mutants of dynamin and Eps15 prevents HIV-1 entry into TZM-bl cells (5–7). Furthermore, shRNA screening identified host factors involved in endocytosis as dependency factors for HIV-1 fusion with a CEM-derived cell line (8). However, whether endocytosis plays a role in productive HIV-1 entry into primary CD4$^+$ T cells, which are the primary target of HIV-1, is still debated due to the contrasting results obtained with this cell type (9–15).

The membrane-impermeable HIV-1 fusion inhibitor, T-20, completely blocks HIV-1 entry into primary CD4$^+$ T cells, even if its addition is delayed after incubation with HIV-1 at 22 °C that allows for substantial endocytosis but not fusion (15). This suggests that the plasma membrane is the site of HIV-1 entry into primary CD4$^+$ T cells. In contrast to this observation, studies in which the T cells were inoculated at 37 °C showed that HIV-1 entry into primary CD4$^+$ T cells does occur at a surface inaccessible compartment, e.g., endosomal compartments (13, 14). These studies demonstrated the presence of a virus population that is susceptible to the temperature block at 4 °C, which inhibits virus fusion regardless of subcellular location, but is resistant to treatment with fusion inhibitors or protease, which can target only cell-surface fusion events. Consistent with this, a very recent study using live-cell imaging techniques reported that HIV-1 fusion with primary CD4$^+$ T cells occurs at neutral pH endosomal compartments (12). Collectively, these findings suggest that HIV-1 can enter primary CD4$^+$ T cells via endocytic pathway(s) that are likely to be active at 37 °C but not 22 °C. However, which endocytic pathway mediates HIV-1 entry into primary CD4$^+$ T cells remains to be determined.

There are multiple endocytic pathways, e.g., clathrin-mediated endocytosis, non-clathrin-mediated endocytosis, and macropinocytosis (16). Macropinocytosis is a

Author contributions: T.M. and A.O. designed research; T.M., R.d.S.C., P.M., K.-N.C., and Y.T. performed research; T.M., P.M., Y.-T.C., and E.R. contributed new reagents/analytic tools; T.M., R.d.S.C., and E.R. analyzed data; J.A.S., P.D.K., and A.O. supervised and coordinated research; and T.M., J.A.S., P.D.K., and A.O. wrote the paper.

The authors declare no competing interest.

This article is a PNAS Direct Submission.

Copyright © 2025 the Author(s). Published by PNAS. This open access article is distributed under Creative Commons Attribution-NonCommercial-NoDerivatives License 4.0 (CC BY-NC-ND).

[1]To whom correspondence may be addressed. Email: tmurakam@umich.edu, kingp@umich.edu, or akiraono@umich.edu.

This article contains supporting information online at https://www.pnas.org/lookup/suppl/doi:10.1073/pnas.2417676122/-/DCSupplemental.

Published June 4, 2025.

large-scale and actin-dependent fluid phase form of endocytosis (16, 17). Macropinocytosis is important for sustaining mTORC activity (17–20). It is well known that macrophages, dendritic cells, and cancer cells engage in macropinocytosis (20). Notably, macropinocytosis is implicated in HIV-1 entry into macrophages, endothelial cells, and epithelial cells (21–24). In addition to HIV-1, the entry step of other viruses including ebolavirus, influenza A virus, vaccinia virus, and SARS-CoV-2 is mediated by macropinocytosis (25–29). Recently, our group made the surprising discovery that primary $CD4^+$ T cells also engage in macropinocytosis, despite their relative paucity of cytoplasm (17, 19). This, therefore, raises the possibility that HIV-1 could infect primary $CD4^+$ T cells through a macropinocytic route. However, whether macropinocytosis in primary $CD4^+$ T cells promotes HIV-1 entry into this cell type has not been explored.

In this study, using engineered HIV-1 constructs whose fusion is reversibly arrested, we showed that HIV-1 entry into primary $CD4^+$ T cells, but not common T cell lines, can take place at endosomal compartments. We also observed that an inhibitor of macropinocytosis suppressed HIV-1 internalization into and subsequent fusion with primary $CD4^+$ T cells. Furthermore, we demonstrated the presence of internalized HIV-1 particles in macropinosomes, defined here as macropinocytosis-derived vesicles, and their fusion at macropinosomes in primary $CD4^+$ T cells. Finally, an inhibitor of macropinocytosis prevented HIV-1 infection of primary $CD4^+$ T cells. These findings indicate that macropinocytosis enhances HIV-1 infection of primary $CD4^+$ T cells via mediating HIV-1 internalization and fusion.

Results

HIV-1 Entry Occurs Both at the Plasma Membrane and Endosomal Compartments in Primary $CD4^+$ T Cells. To investigate whether productive HIV-1 entry into primary $CD4^+$ T cells takes place at endosomal compartments, we examined the sensitivity of HIV-1 encoding the SOS Env protein, which has an engineered disulfide bond between gp120 and gp41 subunits (30–32), to a fusion inhibitor added after inoculation. The fusion process of HIV-1 with SOS Env proceeds up to the interactions of gp120 with CD4 and coreceptors. However, the engineered disulfide bond in SOS Env arrests the subsequent process by preventing gp120 dissociation from gp41. Addition of a reducing agent, DTT, dissociates gp120 and gp41 and thereby allows the remaining fusion steps to occur. Since DTT is membrane permeable, it can induce the fusion of HIV-1 SOS Env regardless of the site of HIV-1 fusion, i.e., both at the plasma membrane and internalized compartments. To distinguish the sites of virus-cell fusion, we used a peptide-based HIV-1 fusion inhibitor, T-20, which inhibits six-helix bundle formation. T-20 can block HIV-1 fusion at the plasma membrane. However, since T-20 is membrane impermeable (33), this drug cannot prevent the fusion at endosomal compartments that are already formed at the time of addition. The combined use of HIV-1 SOS Env, DTT, and T-20 allows us to determine the fraction of HIV-1 entry that occurs at endosomal compartments. An HIV-1 integrase inhibitor, raltegravir (Ral), was used as a positive control because Ral blocks HIV-1 infection regardless of the site of HIV-1 fusion. Activated primary $CD4^+$ T cells and two T cell lines frequently used in HIV-1 studies (A3.01 cells and Jurkat cells) were inoculated with CXCR4-using HIV-$1_{NL4\text{-}3/SOS\ Env}$ encoding NanoLuc for 2 h at 37 °C and treated with DTT for 10 min at 22 to 23 °C. At this temperature, the fusion process is arrested at the formation of a prehairpin intermediate (34). Cells were then incubated or not with Ral or T-20 for 15 min at 22 to 23 °C and then further cultured for 3 d at 37 °C. Additionally, an HIV-1 protease inhibitor, saquinavir (SQV), was added to completely inhibit the unexpected multiple-cycle replication, if any, of the SOS Env-encoding virus during the culture for 3 d. Cells were lysed, and the NanoLuc activity in the lysates was measured and normalized by the total protein amounts (Fig. 1*A*). Although the DTT treatment reduced the total protein amounts by approximately 20% in primary $CD4^+$ T cells compared to nontreated cells, neither Ral nor T-20 affected the total protein amounts in DTT-treated cells (*SI Appendix*, Fig. S1*A*). As expected, DTT induced the infection of CXCR4-using HIV-$1_{NL4\text{-}3/SOS\ Env}$ of primary $CD4^+$ T cells, which was inhibited by Ral. T-20 was statistically significantly less efficient than Ral in inhibiting HIV-1 infection of primary $CD4^+$ T cells isolated from most donors (Fig. 1*B* and *SI Appendix*, Fig. S1*B*), indicating that at least a part of virus-cell fusion takes place at an internal compartment. In contrast, both Ral and T-20 significantly inhibited HIV-1 infection of A3.01 cells and Jurkat cells to a similar extent (Fig. 1 *C* and *D*). These results demonstrate that HIV-$1_{NL4\text{-}3/SOS\ Env}$ entry into primary $CD4^+$ T cells can take place at two locations, i.e., at the plasma membrane and internal compartments. In contrast, the plasma membrane is the primary site of HIV-1 entry into A3.01 cells and Jurkat cells.

Macropinocytosis Inhibitors Suppress Total HIV-1 Internalization Into Primary $CD4^+$ T Cells. While a previous study showed that endocytosis that is active at 22 ºC does not mediate HIV-1 entry into primary $CD4^+$ T cells (15), our results suggest that endocytosis taking place at 37 °C plays a role in HIV-1 infection of primary $CD4^+$ T cells (Fig. 1). Our group previously demonstrated that primary $CD4^+$ T cells engage in macropinocytosis, a fluid-phase endocytosis by which large molecules are preferentially internalized (17, 19). To determine whether macropinocytosis in primary $CD4^+$ T cells is active at 22 °C, we measured macropinocytosis activity at 4, 22, and 37 °C by using a macropinocytosis cargo, BSA. Whereas we observed BSA uptake at 37 °C, primary $CD4^+$ T cells did not show efficient uptake at 4 and 22 °C (*SI Appendix*, Fig. S2 *A* and *B*). This result indicates that macropinocytosis is active at 37 °C but not at 4 and 22 °C.

To investigate whether macropinocytosis is involved in HIV-1 internalization into primary $CD4^+$ T cells, we examined the effect of a macropinocytosis specific inhibitor, EIPA (35). Previously, we observed that 50 μM EIPA shows approximately 90% reduction in macropinocytosis in murine $CD4^+$ T cells. By contrast, 10 μM EIPA reduced macropinocytosis activity by only about 10% compared to nontreated cells (19). Treatment of activated human primary $CD4^+$ T cells with 50 μM EIPA for 2 h and 15 min did not affect cell viability (*SI Appendix*, Fig. S3*A*) but significantly reduced macropinocytosis, as measured by the uptake of fluorescent BSA. To examine the effect of EIPA on HIV-1 internalization, we constructed HIV-1 molecular clones encoding the Gag protein with a NanoLuc insertion between MA and CA domains (Gag-iNanoLuc). This virus incorporates NanoLuc into virions. Activated primary $CD4^+$ T cells and A3.01 cells were pretreated or not with EIPA or T-20 for 15 min and inoculated with the virus for 2 h at 37 °C in the absence or presence of the compounds. Cells were then washed, trypsinized to remove surface-bound viruses for 1 h at 4 °C, and lysed to determine the intracellular NanoLuc activity. Upon HIV-1 fusion, viral contents are released to the cytosol of target cells. Since NanoLuc is a content of virions, the NanoLuc activity in cell lysates should indicate the sum of HIV-1 endocytosis and fusion at the cell surface in this experimental setting. To investigate the contribution of the cell surface-fused HIV-1 to the NanoLuc activity, we used T-20, which inhibits the fusion at the cell surface but not endocytosis of virus particles (Fig. 2*A*). When cells were inoculated at 4 °C, at which

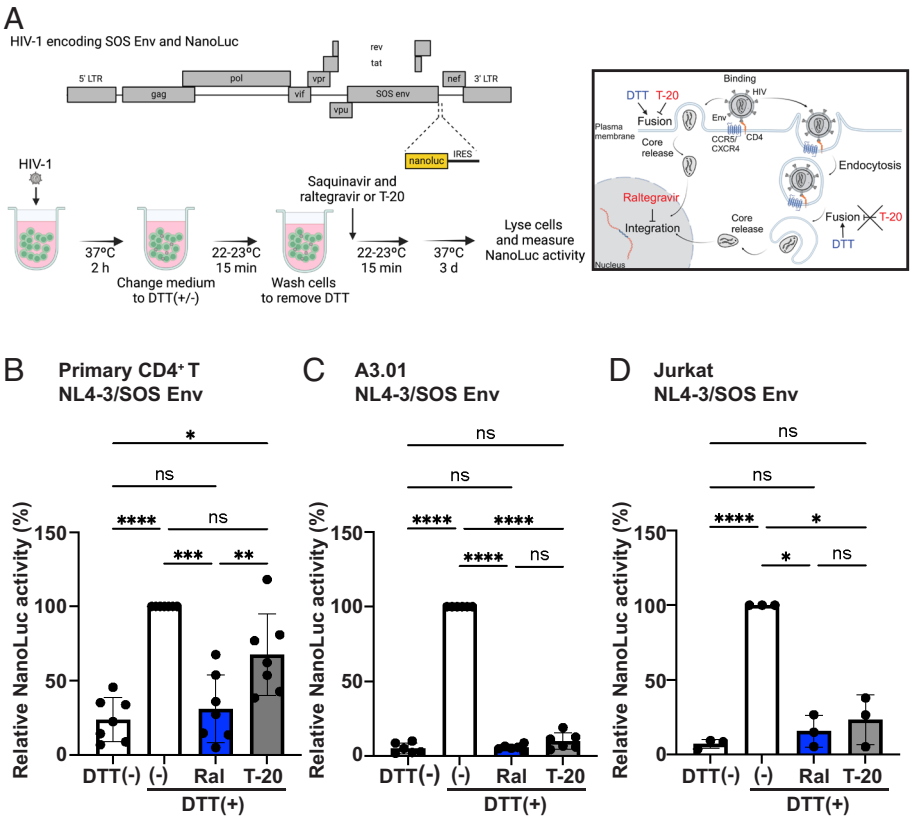

Fig. 1. HIV-1 entry into primary CD4$^+$ T cells takes place at both the plasma membrane and internalized compartments. (*A*) Schematic illustrations of the experimental procedure. Cells were inoculated with HIV-1 molecular clones encoding SOS Env at 37 °C for 2 h. Inoculated cells were incubated for 10 min at room temperature (22 to 23 °C) in the presence and absence of DTT and washed to remove DTT. Cells were then incubated for 15 min at room temperature and further cultured at 37 °C in the presence of saquinavir and either raltegravir, T-20, or vehicles. After 3 d, the NanoLuc activity in cell lysates was measured and normalized by total protein amounts. (*B–D*) Activated primary CD4$^+$ T cells, A3.01 cells, and Jurkat cells were used as target cells. Indicated cells were inoculated with indicated viral strains. Data are presented as means ±SD. The experiments were performed seven times with primary CD4$^+$ T cells isolated from seven donors in *B*, six times with A3.01 cells in *C*, and three times with Jurkat cells in *D*. The *P* values were determined using Tukey's test following one-way ANOVA. *$P < 0.05$; **$P < 0.01$; ***$P < 0.001$; ****$P < 0.0001$; n.s., not significant.

temperature HIV-1 attaches to the plasma membrane but does not undergo endocytosis and fusion, trypsinization for 1 h at 4 °C removed approximately 90% of HIV-1 from cells compared to those without trypsinization (*SI Appendix*, Fig. S4*A*). This result indicates that trypsin treatment removes almost all surface-bound viruses. When primary CD4$^+$ T cells were inoculated with CXCR4-using HIV-$1_{NL4\text{-}3/Gag\text{-}iNanoLuc}$ at 37 °C, both EIPA and T-20 reduced the intracellular NanoLuc activity compared to nontreated cells (Fig. 2*B*). The NanoLuc signal detected in the presence of T-20 is likely due to internalization of fusion-arrested particles via endocytosis. In contrast to primary CD4$^+$ T cells, the intracellular NanoLuc activity in A3.01 cells was sensitive to only T-20 and completely insensitive to EIPA (Fig. 2*C*), even though EIPA reduces macropinocytosis in A3.01 cells (*SI Appendix*, Fig. S3*D*). Considering that T-20 is not known to inhibit endocytosis, the reduction in the NanoLuc activity in A3.01 cells is likely due to the inhibitory effect of T-20 on cell surface fusion, thereby increasing the trypsin-accessible virus population. The effect of EIPA on intracellular NanoLuc activity in primary CD4$^+$ T cells was not limited to CXCR4-dependent HIV-1. We observed that compared to T-20, EIPA efficiently suppressed intracellular NanoLuc activity of primary CD4$^+$ T cells inoculated with CCR5-using HIV-$1_{NL4\text{-}3/Gag\text{-}iNanoLuc/CH040env}$ in which the env sequence of HIV-$1_{NL4\text{-}3/Gag\text{-}iNanoLuc}$ was replaced with that of CH040 (Fig. 2*D*). Furthermore, in the same condition, we found that EIPA inhibits internalization of unmodified HIV-$1_{NL4\text{-}3}$ into primary CD4$^+$ T cells (*SI Appendix*, Fig. S4*B*). EIPA did not affect CD4 density on the surface of primary CD4$^+$ T cells (*SI Appendix*, Fig. S5 *A* and *B*), suggesting that the EIPA treatment is unlikely to affect HIV-1 attachment to target cells through CD4. Considering that the macropinocytosis activity measured by BSA uptake is inhibited approximately 40 to 50% at the concentration of EIPA used in these experiments (*SI Appendix*, Fig. S3*C*), the 30 to 50% reduction in the intracellular NanoLuc activity in EIPA-treated primary CD4$^+$ T cells (Fig. 2 *B* and *D*) is significant. These results strongly suggest that while EIPA-insensitive macropinocytosis and/or nonmacropinocytic endocytosis play a role in HIV-1 internalization into both primary CD4$^+$ T cells and A3.01 cells, EIPA-sensitive macropinocytosis contributes to HIV-1 internalization specifically into primary CD4$^+$ T cells but not A3.01 cells and in a manner independent of the coreceptor usage. To validate the observations obtained with the EIPA treatment, we examined the effect of jasplakinolide in combination with blebbistatin (J/B), which we showed inhibits macropinocytosis in primary CD4$^+$ T cells in our previous study (19). We found that J/B treatment does not affect CD4 density on primary CD4$^+$ T cells (*SI Appendix*, Fig. S5*C*) but significantly inhibited intracellular NanoLuc activity of primary CD4$^+$ T cells inoculated with HIV-$1_{NL4\text{-}3/Gag\text{-}iNanoLuc}$ (*SI Appendix*, Fig. S5*D*). Altogether, these results suggest that inhibition of macropinocytosis suppresses HIV-1 internalization into primary CD4$^+$ T cells.

Macropinocytosis Inhibitors Attenuate HIV-1 Entry Into the Cytoplasm of Primary CD4$^+$ T Cells. To test whether EIPA prevents cytoplasmic HIV-1 entry, we performed the BlaM-Vpr-based fusion assay (36), which measures the amount of virion-incorporated BlaM-Vpr released into the cytosol upon HIV-1 fusion with target cells. The β-lactamase activity of BlaM-Vpr in

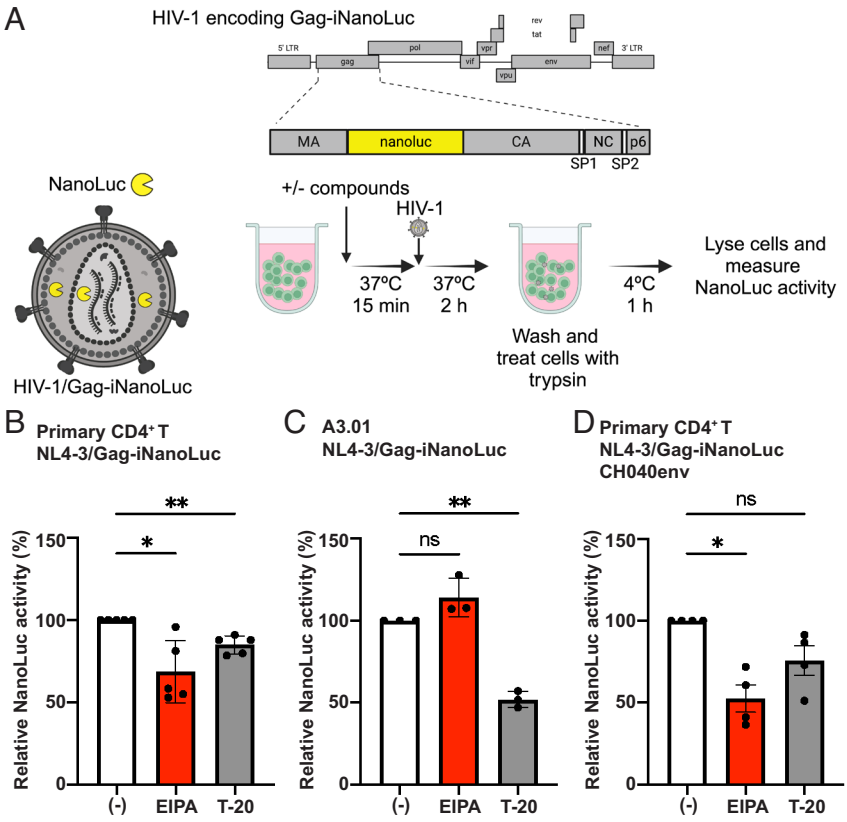

Fig. 2. A macropinocytosis inhibitor inhibits total HIV-1 internalization into primary CD4$^+$ T cells. (*A*) A schematic illustration of the experimental procedure performed for panels (*B–D*). Activated primary CD4$^+$ T cells and A3.01 cells were pretreated with either EIPA, T-20, or vehicles for 15 min at 37 °C and inoculated with HIV-1 molecular clones for 2 h in the presence or absence of either EIPA or T-20. The NanoLuc activity in cell lysates was measured and normalized by total protein amounts. (*B–D*) Indicated cells were inoculated with indicated viral strains. Data are presented as means ±SD. The experiments were performed with primary CD4$^+$ T cells isolated from five (*B*) and four (*D*) donors, respectively, in three independent experiments and with A3.01 cells (*C*) in three independent experiments. The *P* values were determined using Dunnett's test following one-way ANOVA. *$P < 0.05$; **$P < 0.01$; n.s., not significant.

target cells loaded with the cytosolic substrate CCF2 correlates with the efficiency of HIV-1 content release into the cytosol of target cells (Fig. 3*A*). Activated primary CD4$^+$ T cells and A3.01 cells were pretreated with the inhibitors, inoculated with HIV-1 containing BlaM-Vpr, loaded with CCF2-AM, and labeled with an anti-CXCR4 or CCR5 antibody. The efficiency of the cytoplasmic entry of HIV-1 (measured as the "fusion" efficiency) and the expression of CXCR4 and CCR5 were analyzed by flow cytometry. We observed approximately 20 to 25% of reduction in CXCR4 density on the surface of both primary CD4$^+$ T cells and A3.01 cells treated with EIPA compared to nontreated cells (Fig. 3 *B–D*). Although EIPA suppressed HIV-1_{NL4-3} fusion with both CXCR4$^+$ primary CD4$^+$ T cells and A3.01 cells, primary CD4$^+$ T cells were more sensitive to EIPA than A3.01 cells (approximately 50% reduction versus 25%; Fig. 3 *E–G*). To determine whether the reduction in CXCR4 density on the surface of primary CD4$^+$ T cells fully explains the suppression of HIV-1_{NL4-3} fusion with CXCR4$^+$ primary CD4$^+$ T cells, we compared fusion efficiency in nontreated and EIPA-treated cells that expressed the same amounts of CXCR4, as observed among CXCR4 low expressing cells in both populations (*SI Appendix*, Fig. S6 *A* and *B*). In this comparison, EIPA-treated primary CD4$^+$ T cells still showed lower HIV-1_{NL4-3} fusion than untreated cells (*SI Appendix*, Fig. S6 *C* and *D*), indicating that the reduction in surface expression of CXCR4 by EIPA does not fully explain the inhibitory effect of EIPA on HIV-1_{NL4-3} fusion with primary CD4$^+$ T cells. Consistent with this observation, EIPA also suppressed HIV-1_{CH040} fusion with CCR5$^+$ primary CD4$^+$ T cells without affecting CCR5 density on the surface of the cells (Fig. 3 *H–J*). These results indicate that EIPA attenuates content release of HIV-1 into the cytoplasm of primary CD4$^+$ T cells independently of the coreceptor usage. Likewise, J/B inhibited HIV-1_{NL4-3} fusion with primary CD4$^+$ T cells without inhibitory effects on CXCR4 expression (*SI Appendix*, Fig. S7 *A* and *B*). Taken together, these results strongly suggest macropinocytosis contributes to cytoplasmic entry of HIV-1 into primary CD4$^+$ T cells.

A Microscopy Analysis Displays Macropinocytosis-Mediated HIV-1 Particle Internalization Into Primary CD4$^+$ T Cells. The enzyme-based bulk cell analyses described above support the involvement of macropinocytosis in HIV-1 internalization into and fusion with primary CD4$^+$ T cells (Figs. 2 and 3). To test whether HIV-1 particles are internalized through macropinocytosis in primary CD4$^+$ T cells, we performed microscopic analyses using HIV-$1_{NL4-3/Gag-iVenus}$ containing mScarlet-Vpr. Labeling of HIV-1 particles with two fluorescent proteins allowed us to distinguish unambiguously HIV-1 particles from CD4$^+$ T cell–derived autofluorescent punctate signals, which are either in red or green fluorescence but not both. Activated primary CD4$^+$ T cells were pretreated or not with EIPA or T-20 and inoculated with double-labeled HIV-1 in the presence of BSA-AlexaFluor647 for 1 h at 37 °C, washed, trypsinized to remove surface-bound HIV-1 particles, and immunostained with an anti-CD4 antibody conjugated with a fluorescent dye, BV421. Cells were then fixed and observed using a spinning-disk confocal microscope (Fig. 4*A*). Visualization of the inocula showed that approximately 88% of HIV-$1_{NL4-3/Gag-iVenus}$ contained mScarlet-Vpr (*SI Appendix*, Fig. S8*A*). HIV-$1_{NL4-3/Gag-iVenus}$ containing mScarlet-Vpr showed

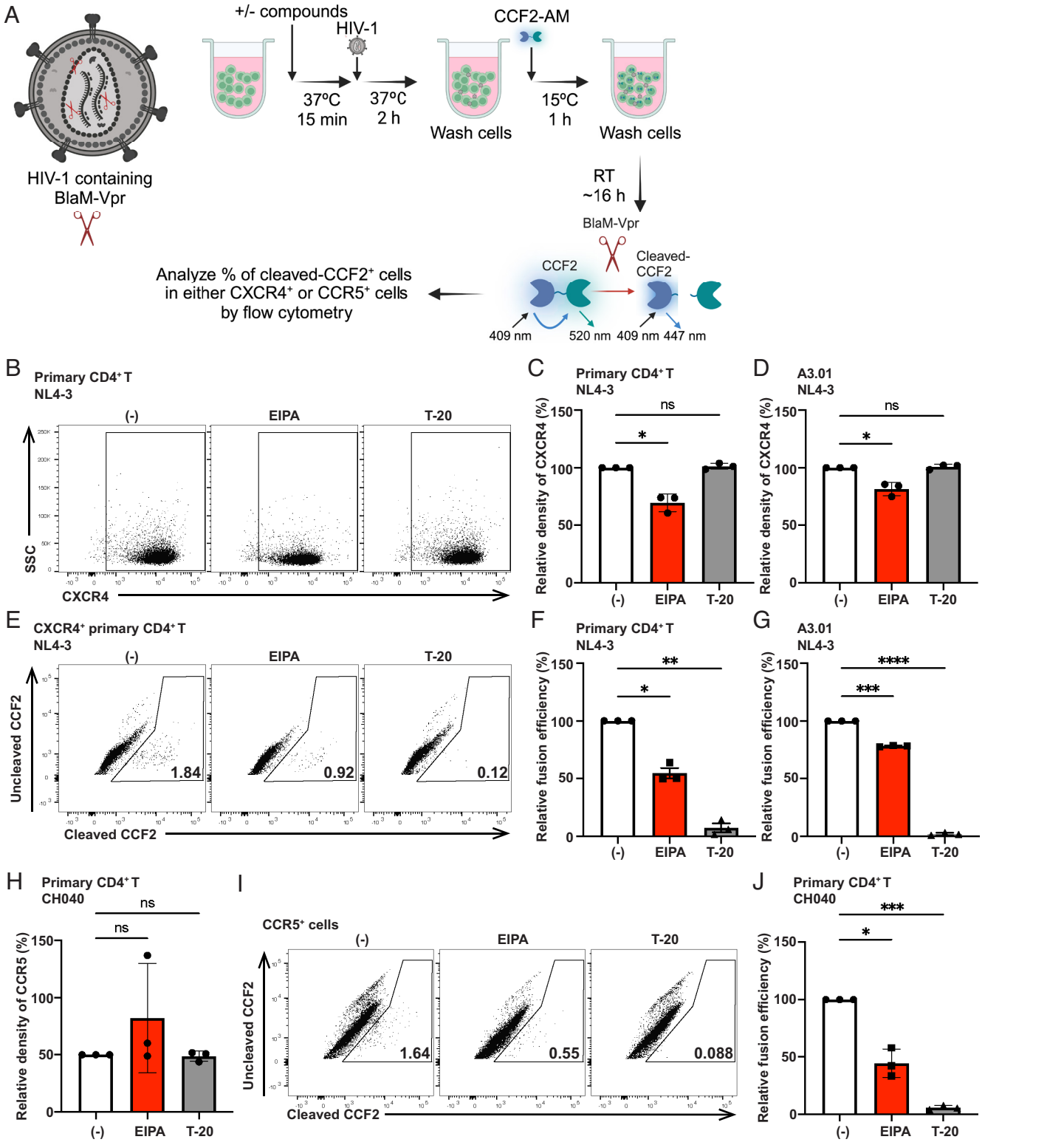

Fig. 3. A macropinocytosis inhibitor inhibits HIV-1 fusion with primary CD4$^+$ T cells. (*A*) A schematic illustration of the experimental procedure performed for panels (*B–J*) Activated primary CD4$^+$ T cells and A3.01 cells were pretreated with either EIPA or T-20 or left untreated for 15 min at 37 °C and inoculated with HIV-1 containing BlaM-Vpr for 2 h at 37 °C. Inoculated cells were loaded with CCF2-AM at 15 °C for 1 h and incubated overnight at room temperature. The cells were then labeled with either an anti-CXCR4-APC/Cy7 or CCR5-APC/Cy7 antibody and analyzed by flow cytometry. (*B*) Representative flow plots of surface expression of CXCR4 on primary CD4$^+$ T cells. (*C* and *D*) Quantification of the relative density of surface CXCR4 on primary CD4$^+$ T cells (*C*) and A3.01 cells (*D*). (*E*) Representative flow plots of the percentages of cleaved CCF2$^+$ cells in CXCR4$^+$ cells are shown. (*F* and *G*) Quantification of the relative percentages of cleaved CCF2$^+$ cells (fusion efficiency) in CXCR4$^+$ primary CD4$^+$ T cells (*F*) and A3.01 cells (*G*). (*H*) Quantification of the relative density of surface CCR5 on primary CD4$^+$ T cells. (*I*) Representative flow plots with the percentages of cleaved CCF2$^+$ cells in CCR5$^+$ cells are shown. (*J*) Quantification of the relative percentages of cleaved CCF2$^+$ cells (fusion efficiency) in CCR5$^+$ primary CD4$^+$ T cells. Data are presented as mean ±SD in *C*, *D*, *F–H*, and *J*. The experiments were performed three times with primary CD4$^+$ T cells isolated from three donors in *B*, *C*, *E*, *F*, and *H–J*. The experiments were performed three times with A3.01 cells independently in *D* and *G*. The *P* values were determined using Dunnett's test following one-way ANOVA in *C*, *E–G*. *$P < 0.05$; **$P < 0.01$; ***$P < 0.001$; ****$P < 0.0001$; n.s., not significant.

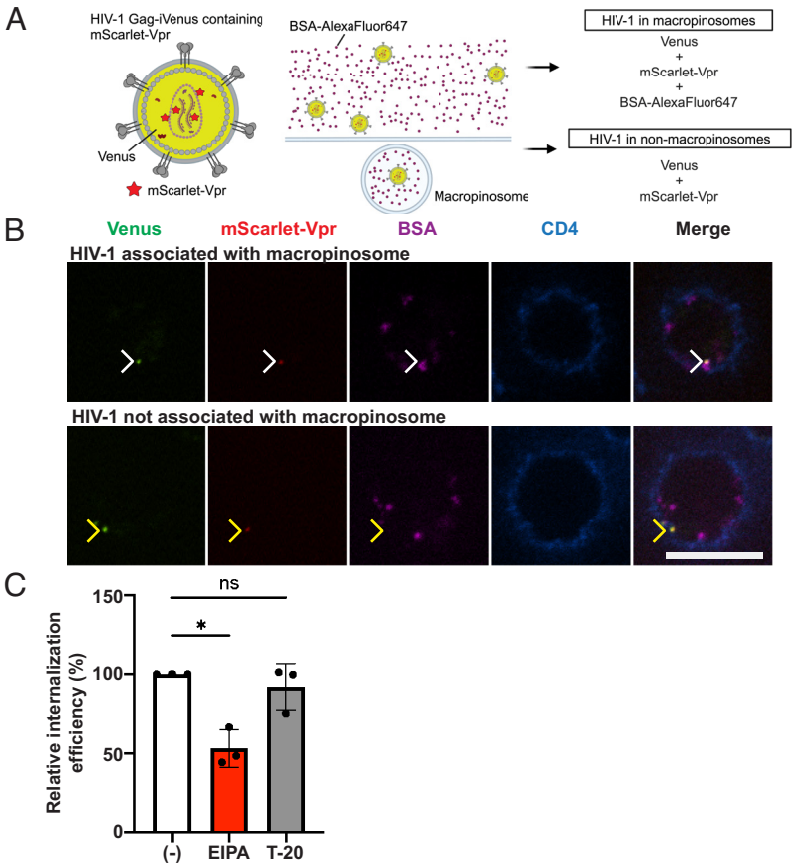

Fig. 4. Observation of macropinocytosis-mediated HIV-1 internalization into primary CD4$^+$ T cells by a microscopic analysis. (*A*) A schematic illustration of the experimental procedure performed for panels *B* and *C*. Activated primary CD4$^+$ T cells were pretreated with either EIPA, T-20, or vehicles for 15 min at 37 °C and inoculated with HIV-$1_{NL4\text{-}3/Gag\text{-}iVenus}$ containing mScarlet-Vpr in the presence of BSA-AlexaFluor647 and in the presence or absence of either EIPA or T-20. Inoculated cells were trypsinized, labeled with an anti-CD4 antibody conjugated with BV421, plated on top of a poly-L-lysine-coated glass bottom chamber, and fixed. The fixed cells were observed with a spinning-disk confocal microscope. (*B*) Examples of internalized Venus- and Vpr-positive HIV-1 particles detected in individual *z*-slices of cells treated with vehicles are shown. White and yellow arrowheads indicate an HIV-1 particle colocalized with BSA-AlexaFluor647 ("HIV-1 in macropinosomes") and an HIV-1 particle not colocalized with BSA-AlexaFluor647 ("HIV-1 in nonmacropinosomes"), respectively. Bar, 10 μm. (*C*) Quantification of the relative internalization efficiency. The punctate signals for internalized HIV-1 in macropinosomes (panel *B*) were quantified and normalized with cell numbers. A total of more than 51 cells in each condition were examined in each of three independent experiments. The *P* values were determined using Dunnett's test following one-way ANOVA. *$P < 0.05$; n.s., not significant.

reduced but still substantial infectivity relative to HIV-$1_{NL4\text{-}3}$ (*SI Appendix*, Fig. S8*B*). We observed colocalization of ~55% of HIV-1 particles with BSA-AlexaFluor647 (Fig. 4*B*, white arrowheads). The EIPA treatment prevented the uptake of BSA-AlexaFluor647, resulting in significantly suppressed colocalization of HIV-1 particles with BSA-AlexaFluor647 (Fig. 4 *B* and *C*). HIV-1 internalization via macropinocytosis was insensitive to T-20 (Fig. 4*C*), which is consistent with the notion that fusion-arrested virus particles can be endocytosed (Fig. 2). These results indicate that both macropinocytosis and nonmacropinocytic endocytosis serve as a pathway for HIV-1 internalization into primary CD4$^+$ T cells and suggest that EIPA dampens HIV-1 internalization through macropinocytosis into primary CD4$^+$ T cells.

A Microscopy Observation Showed HIV-1 Fusion at Macropinosomes in Primary CD4$^+$ T Cells. Even though it has been reported that HIV-1 fusion takes place at endosomal compartments in primary CD4$^+$ T cells (12–14), which endocytic pathway(s) mediate HIV-1 fusion is unknown. To investigate whether HIV-1 fusion takes place at macropinosomes, we attempted to use HIV-$1_{NL4\text{-}3}$ with membranes labeled by lipophilic dyes, R18 and DiOC18. It has been reported that influenza virus labeled with this combination allows for detection of the subcellular fusion sites based on the increase in emission of the DiOC18 fluorescence due to dye dequenching (37). We observed the colocalization of macropinosomes and labeled HIV-1 in primary CD4$^+$ T cells in two independent experiments. However, in the two different conditions that we examined, we observed the dequenching of DiOC18 at macropinosomes even in the presence of a fusion inhibitor, AMD3100 (*SI Appendix*, Fig. S9). Although these results indicate that nonengineered HIV-1 is internalized into primary CD4+ T cells via macropinosomes, they also suggest that this labeling method is not applicable to examine the site of HIV-1 fusion. As an alternative approach, we decided to use HIV-$1_{NL4\text{-}3/MA\text{-}3xHA}$, which encodes three copies of an HA-tag near the C terminus of the MA domain of Gag (MA-3xHA) (38) (Fig. 5*A*). Since MA should remain at sites of HIV-1 fusion because of its membrane-binding ability (39), the HA signal associated with macropinosomes would represent either the fusion at the macropinosomes or prefusion virus particles therein. The insertion of 3xHA within the C-terminal region of MA did not affect virus assembly, release, and maturation (*SI Appendix*, Fig. S10). The infectivity of HIV-$1_{NL4\text{-}3/MA\text{-}3xHA}$ was approximately 60% of that of HIV-$1_{NL4\text{-}3}$ (*SI Appendix*, Fig. S8*B*). Activated CD4$^+$ T cells were inoculated for 2 h with HIV-$1_{NL4\text{-}3/MA\text{-}3xHA}$ in the presence of BSA-AlexaFluor488 and in the presence or absence of T-20. CD4 on the surface of cells was labeled to identify the cell surface. To detect the postfusion MA-3xHA, which should be exposed at the cytoplasmic side of the macropinosome membrane, while minimizing the detection of prefusion viruses inside macropinosomes, we treated the fixed cells with a very low concentration of digitonin to permeabilize only the

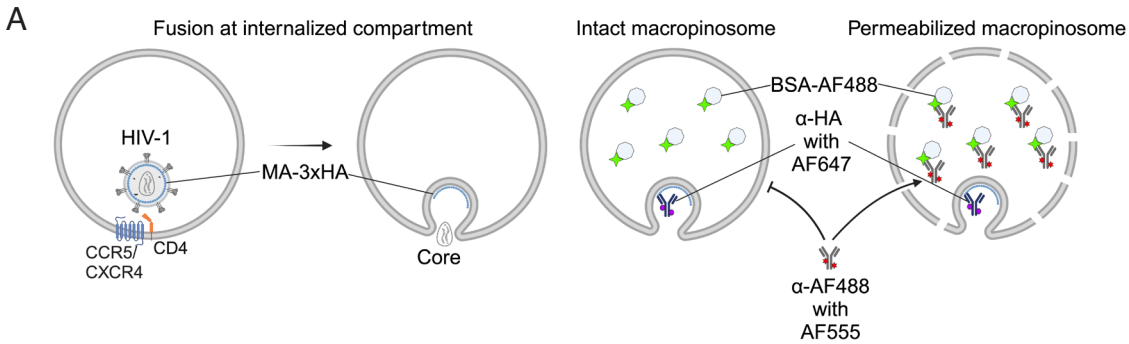

Classification	AF647 (Magenta)	AF488 (Green)	AF555 (Red)
a) MA-3xHA associated with permeabilized macropinosomes	+	+	+
b) MA-3xHA associated with intact macropinosomes	+	+	-
c) MA-3xHA not associated with macropinosomes	+	-	-

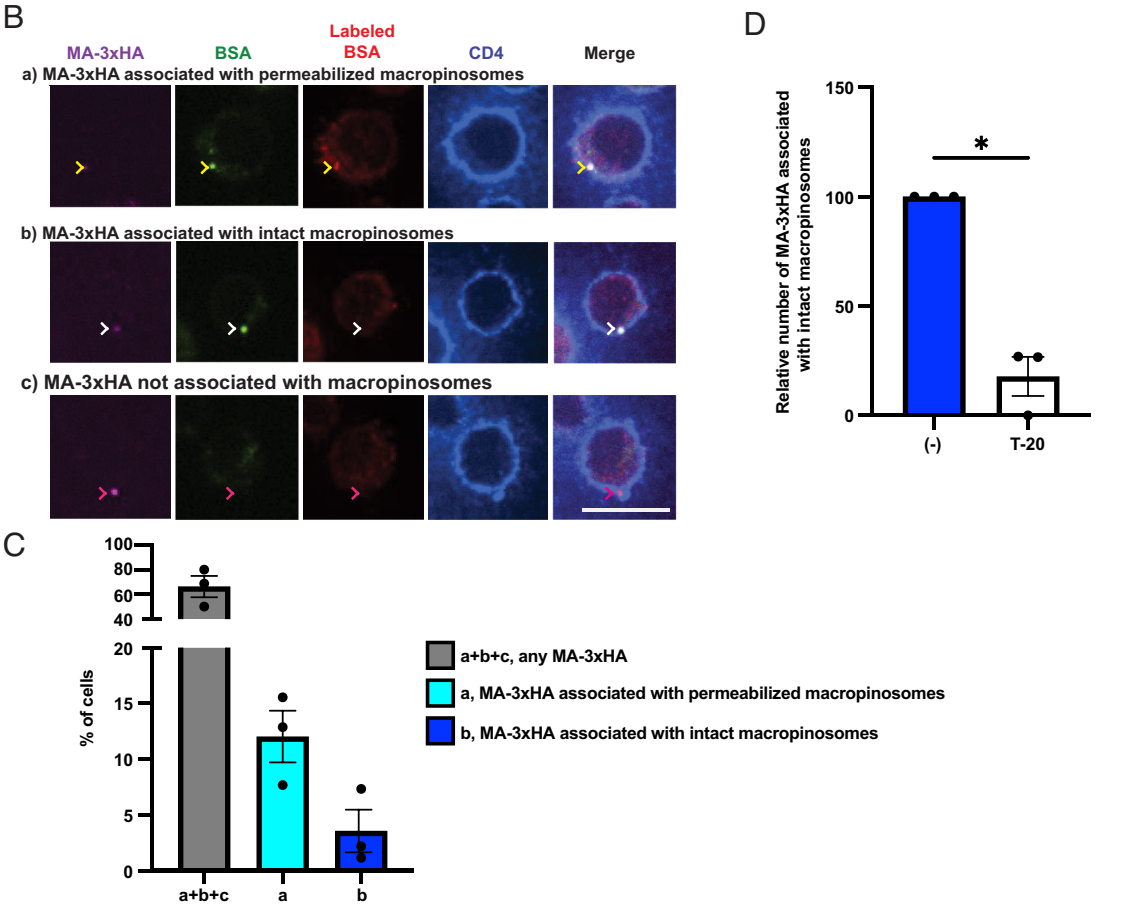

Fig. 5. HIV-1 fusion occurs at macropinosomes in primary CD4$^+$ T cells. (*A*) A schematic illustration of the experimental procedure performed for panels *B* and *C*. Activated primary CD4$^+$ T cells were inoculated with HIV-1$_{NL4\text{-}3/MA\text{-}3xHA}$ in the presence of BSA-AlexaFluor488. Cells were labeled with an anti-CD4 antibody conjugated with BV421, plated on top of a poly-L-lysine-coated glass bottom chamber, and fixed. The fixed cells were permeabilized with digitonin and labeled with an anti-AlexaFluor488 antibody followed by the secondary antibody conjugated with AlexaFluor555 and an anti-HA antibody conjugated with AlexaFluor647. The cells were observed with a spinning-disk confocal microscope. (*B*) Individual *z*-slices of representative cells are shown. Yellow arrowheads indicate MA-3xHA signals colocalized with BSA-AlexaFluor488 and AlexaFluor555 (permeabilized macropinosome with MA-3xHA), white arrowheads indicate MA-3xHA signals colocalized with BSA-AlexaFluor488 without AlexaFluor555 (intact macropinosome with MA-3xHA), and pink arrowheads indicate MA-3xHA signals colocalized with neither BSA-AlexaFluor488 nor AlexaFluor555. (Scale bar, 10 μm.) (*C*) Quantification of the percentages of cells with any MA-3xHA, a + b + c; MA-3xHA associated with permeabilized macropinosomes, a; and MA-3xHA associated with intact macropinosomes, b. (*D*) Quantification of the number of MA-3xHA puncta associated with intact macropinosomes. The number of MA-3xHA puncta was normalized with cell numbers. The experiments were performed three times with primary CD4$^+$ T cells isolated from three donors. A total of more than 134 cells were examined in each of three independent experiments. The *P* values were determined using two-tailed paired Student's *t* test. *$P < 0.05$.

plasma membrane but not the macropinosome and viral membranes prior to immunostaining with an anti-HA antibody conjugated with AlexaFluor647. Nonetheless, since both macropinosome and viral membranes originate from the plasma membrane, it is possible that digitonin permeabilizes those membranes in addition to the plasma membrane, thereby making MA-3xHA in prefusion virus particles within macropinosomes accessible to the anti-HA antibody. To distinguish MA-3xHA present at the cytoplasmic side

of macropinosomes (indicating HIV-1 fusion) from MA-3xHA exposed due to permeabilization of both macropinosomes and viral membranes, we used an anti-AlexaFluor488 antibody followed by a secondary antibody conjugated with AlexaFluor555, which will detect BSA-AlexaFluor488 in permeabilized macropinosomes but not intact macropinosomes. Based on distances between the fluorescence signals, which were measured using the Imaris software (*SI Appendix*, Fig. S11), we classified MA-3xHA signals into three groups, a) associated with permeabilized macropinosomes, b) associated with intact macropinosomes, and c) not associated with macropinosomes (Fig. 5 *A* and *B*). We quantified the percentages of total cells with MA-3xHA, cells with MA-3xHA associated with permeabilized macropinosomes, and cells with MA-3xHA associated with intact macropinosomes, i.e., HIV-1 fusion at macropinosomes. Among the total cells examined, ~66% of primary $CD4^+$ T cells displayed MA-3xHA signals, which includes cells showing MA-3xHA signals that do not colocalize with either BSA-AlexaFluor488 or AlexaFluor555 (Fig. 5*B*, MA-3xHA not associated with macropinosomes and Fig. 5*C*, a + b + c). In ~12% of total cells, we observed the association of MA-3xHA with permeabilized macropinosomes (Fig. 5*B*, MA-3xHA associated with permeabilized macropinosomes, and Fig. 5*C*, a), which includes signals representing HIV-1 fusion at macropinosomes and prefusion virus particles therein. Finally, approximately 3.5% of total cells showed the association of MA-3xHA with intact macropinosomes (Fig. 5*B*, MA-3xHA associated with intact macropinosomes, and Fig. 5*C*, b). We also quantify the number of MA-3xHA puncta associated with intact macropinosomes. Importantly, we found that the T-20 treatment inhibited the exposure of MA-3xHA at intact macropinosomes (Fig. 5*D*). These results demonstrated that HIV-1 fusion can occur at macropinosomes in primary $CD4^+$ T cells.

Macropinocytosis Inhibitors Inhibit HIV-1 Infection of Primary $CD4^+$ T Cells. Our group previously showed that macropinocytosis is essential for sustaining mTORC1 activity in $CD4^+$ T cells (17, 19). Additionally, other groups reported that active mTORC1 regulates HIV-1 infection (40–46). Therefore, it is conceivable that inhibition of macropinocytosis can prevent HIV-1 infection through the inhibition of both entry step and mTORC1 activation. We first sought to determine whether EIPA inhibits mTORC1 activity in primary $CD4^+$ T cells. Activated primary $CD4^+$ T cells were treated or not with either EIPA, or AZD2014, which is a specific mTOR inhibitor, or T-20 for 2 h and 15 min at 37 °C. The treatment of primary $CD4^+$ T cells with either EIPA or AZD2014 inhibited the phosphorylation of the S6 protein, indicating that these compounds suppress mTORC1 activity in primary $CD4^+$ T cells (Fig. 6 *A* and *B*). To investigate the effect of these compounds on productive infection by HIV-1, activated primary $CD4^+$ T cells and A3.01 cells were inoculated with a replication-competent HIV-1_{NL4-3} encoding NanoLuc (HIV-1_{NL-NI}) for 2 h at 37 °C in the presence or absence of EIPA, AZD2014, or T-20. Cells were then washed to remove unbound viruses and compounds and further cultured for 24 h at 37 °C in the presence of SQV to prevent multiple-cycle replication (Fig. 6*C*). EIPA but not AZD2014 inhibited HIV-1_{NL-NI} infection of primary $CD4^+$ T cells (Fig. 6*D*). In contrast, neither EIPA nor AZD2014 inhibited HIV-1_{NL-NI} infection of A3.01 cells (Fig. 6*E*), even though EIPA partially inhibited HIV-1 fusion with this cell type (Fig. 3*G*). In addition, the infection of primary $CD4^+$ T cells with a transmitted/founder virus encoding NanoLuc (HIV-$1_{CH040-NI}$) was inhibited by EIPA more efficiently than AZD2014 (Fig. 6*F*). These results indicate that EIPA inhibits HIV-1 infection of primary $CD4^+$ T cells independently of the coreceptor usage. Considering that the inhibitory effect of EIPA on HIV-1 infection was slightly stronger than the effect on HIV-1 internalization and fusion (compare Figs. 2 and 3 versus 6), these results suggest that in addition to HIV-1 entry, EIPA may inhibit other step(s) of HIV-1 replication cycle in primary $CD4^+$ T cells, but it appears unlikely to be a step involving mTORC1 activity. In addition to EIPA, J/B inhibited HIV-1_{NL-NI} infection of primary $CD4^+$ T cells (*SI Appendix*, Fig. S12). Altogether, these results demonstrated that inhibitors of macropinocytosis prevent HIV-1 infection of primary $CD4^+$ T cells.

Discussion

While the contribution of different endocytic pathways to productive infection has been shown (5–8, 12–14), the exact subcellular location of HIV-1 entry into primary $CD4^+$ T cells, which is the major target of HIV-1, remains to be determined. In the present study, we showed using HIV-1 bearing SOS Env that HIV-1 entry into primary $CD4^+$ T cells can take place at both the plasma membrane and internalized compartments. Under the same condition, HIV-1 entered two commonly used T cell lines, A3.01 cells and Jurkat cells, primarily at the plasma membrane. We further observed that EIPA and J/B, macropinocytosis inhibitors, inhibited HIV-1 internalization into, fusion with, and infection of primary $CD4^+$ T cells. We also detected HIV-1 fusion at macropinosomes, endosomes derived from macropinocytosis, in primary $CD4^+$ T cells. Altogether, these results highlight the important role of macropinocytosis in HIV-1 infection of primary $CD4^+$ T cells. This study additionally emphasizes the importance of using primary $CD4^+$ T cells, as opposed to T cell lines, as HIV-1 target cells to elucidate the detailed molecular mechanisms of HIV-1 entry.

Primary $CD4^+$ T cells engage in multiple endocytic pathways, e.g., clathrin-mediated endocytosis, non-clathrin-mediated endocytosis, and macropinocytosis (16). Using microscopic approaches, we demonstrate that macropinocytosis contributes to internalization into and subsequent fusion of HIV-1 with primary $CD4^+$ T cells. This is consistent with the previous observations that are apparently contradictory to each other: one showed that HIV-1 enters into primary $CD4^+$ T cells at the plasma membrane but not endosomes formed at 22 °C (15) and another that HIV-1 entry occurs at endosomal compartments in primary $CD4^+$ T cells (12–14). The observation that macropinocytosis is sensitive to the reduced temperature at which other endocytosis activities can persist (*SI Appendix*, Fig. S2) reconciles the hitherto unresolved discrepancy over the role of endocytosis in HIV-1 infection of primary $CD4^+$ T cells (*Introduction*).

To determine the location of HIV-1 fusion, we used HIV-1 encoding MA-3xHA because MA can remain on the cytoplasmic side of the membrane at the site of fusion (39). In addition, to avoid the detection of prefusion viral particles inside macropinosomes as much as possible, we used digitonin to permeabilize the plasma membrane. This experimental approach has several limitations: i) HIV-1 fusion at the plasma membrane is not detectable because upon HIV-1 fusion with the plasma membrane, MA-3xHA is likely to diffuse laterally from the site of fusion on the plasma membrane, resulting in a loss of signals; ii) The identity of the endosomal compartments associated with MA-3xHA signals not associated with macropinosomes and whether these HA signals represent pre- or postfusion virus cannot be determined; iii) Even though we used very low concentration of digitonin to permeabilize only the plasma membrane, some macropinosomes were permeabilized. Therefore, although MA-3xHA signals associated with intact macropinosomes represent sites of fusion, the fraction of cells with these signals is likely an underestimation of the fusion events at macropinosomes. Additionally, since HIV-1 fusion at the plasma membrane cannot be detected using this

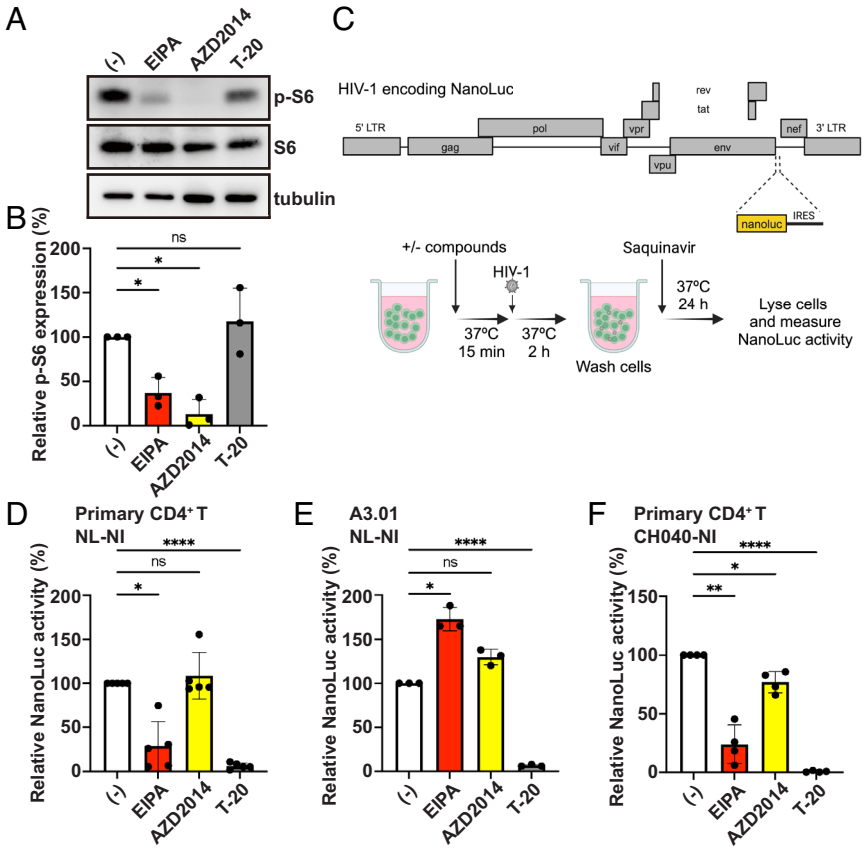

Fig. 6. Inhibition of macropinocytosis diminishes HIV-1 infection of primary CD4$^+$ T cells. (*A*) Analyses of mTORC1 activity by detection of the phosphorylated S6 (p-S6) protein. Activated primary CD4$^+$ T cells were treated with either EIPA, AZD2014, T-20, or vehicles for 2 h and 15 min at 37 °C. Phosphorylated S6, total S6, and tubulin expression in cell lysates was examined by western blotting. The representative images were shown. (*B*) Quantification of the relative expression of the p-S6 normalized by the expression of total S6 protein. (*C*) A schematic illustration of the experimental procedure of *D*–*F*. Activated primary CD4$^+$ T cells and A3.01 cells were pretreated with either EIPA, AZD2014, T-20, or vehicles for 15 min at 37 °C and inoculated with HIV-1 encoding NanoLuc for 2 h at 37 °C. Cells were washed and cultured for 24 h at 37 °C in the presence of saquinavir. Cells were then lysed, and the NanoLuc activity in the cell lysates was measured. The NanoLuc activity was normalized by total protein amounts. (*D* and *F*) Indicated cells were inoculated with indicated viral strains. Data are presented as mean +SD in panel *B* and mean ±SD in panels *D*–*F*, respectively. The experiments were performed with primary CD4$^+$ T cells isolated from three (*A* and *B*), five (*D*), and four (*F*) donors, respectively, in three independent experiments. The experiments were performed three times with A3.01 cells independently in *E*. The *P* values were determined using Dunnett's test following one-way ANOVA in *B*, and *D*–*F*. *$P < 0.05$; **$P < 0.01$; ****$P < 0.0001$; n.s., not significant.

approach, the relative fraction of fusions at macropinosomes versus other locations remains to be determined. Despite these limitations, the results obtained with MA detection in digitonin-permeabilized cells strongly support the notion that HIV-1 fusion occurs in macropinosomes in primary CD4$^+$ T cells. To determine the fraction of HIV-1 fusion that occurs at macropinosomes, live-cell imaging that allows for tracking of internalized particles up to the point of content release should be applied (5, 12, 13) in conjunction with macropinosome markers, such as BSA.

HIV-1 fusion with primary CD4$^+$ T cells was recently reported to take place at endosomes with neutral pH (12). Considering that macropinosomes are acidified during their maturation similar to other endosomes (20, 47), HIV-1 fusion might occur early after macropinocytosis. The acidification of macropinosomes is likely derived from the fusion with lysosomes. In murine bone marrow–derived macrophages, macropinosome-lysosome fusion happens in 7 to 8 min after the formation of the macropinosome (48). This time scale would dovetail with the observation that the half-time for HIV-1 fusion within the neutral-pH endosomes of primary CD4$^+$ T cells is approximately 16 min (12). Nonetheless, it is possible that macropinocytosis in primary CD4$^+$ T cells may differ from that in murine bone marrow–derived macrophages, particularly concerning the timing of acidification. Additionally, there exists the possibility that HIV-1 selectively exploits macropinosomes that evade acidification. Macropinosomes can occasionally recycle back to the plasma membrane without fusing to lysosomes (49), and these macropinosomes might mediate HIV-1 entry into primary CD4$^+$ T cells. Elucidating the properties of macropinosomes containing HIV-1 particles, such as intravesicular pH and their intracellular trafficking pathways, in primary CD4$^+$ T cells is critical for understanding the mechanisms underlying HIV-1 fusion within neutral pH endosomes.

Our experiments using HIV-1 with SOS Env and the membrane-impermeable fusion inhibitor T-20 suggest that the sites of HIV-1 fusion with primary CD4$^+$ T cells are at both the plasma membrane and internal compartments formed at 37 °C. One of the limitations of SOS Env is that the infection efficiency of HIV-1 with SOS Env induced by DTT is unlikely comparable with that of HIV-1 with wild-type Env (50). The accurate comparison of infectivity between wild-type Env and DTT-treated SOS Env in cell-based assays is not feasible because SOS Env requires receptor and coreceptor engagement prior to DTT treatment (30). In addition to this limitation, it is possible that SOS Env-bearing HIV-1 on the surface of target cells can be more efficiently internalized into target cells prior to DTT treatment due to the fusion arrest than HIV-1 with wild-type Env. This potential enhancement of SOS Env-containing HIV-1 internalization may bias our analysis toward overestimation of the fraction of cytoplasmic HIV-1 entry through internalized compartments. Notably, however, at least in this approach, we observed the cell type–specific difference in the

subcellular locations of HIV-1 entry between primary $CD4^+$ T cells and two T cell lines.

There is an apparent discrepancy regarding the results obtained with A3.01 cells. Consistent with the observation obtained with SOS Env (Fig. 1), EIPA does not inhibit productive infection of this cell line by HIV-1 and rather enhances infection (Fig. 6*E*). However, the BlaM-Vpr-based fusion assay demonstrates that EIPA attenuates HIV-1 fusion with A3.01 cells (Fig. 3*G*). This supports the possibility that in A3.01 cells, the EIPA-sensitive fraction of HIV-1 fusion, presumably taking place at macropinosomes, does not contribute to productive infection. Considering that EIPA enhances productive infection of A3.01 cells by HIV-1 without apparent effect on HIV-1 internalization into A3.01 cells as measured by the NanoLuc-based assays (Fig. 2*C*), it is conceivable that in EIPA-treated A3.01 cells, productive fusion at the cell surface is more efficient than in untreated A3.01 cells.

While this manuscript was in preparation, a study reported that EIPA modestly (~40%) inhibits HIV-1 infection of primary $CD4^+$ T cells (12). In the current study, we observed a more robust inhibition of both CXCR4- and CCR5-using HIV-1 infection of primary $CD4^+$ T cells using a similar EIPA treatment protocol (~75%). This difference may be explained by a difference in inoculation procedures: simple inoculation in the current study versus spinoculation in the published study. Spinoculation disrupts the actin cytoskeleton (51). Therefore, spinoculation may have impeded macropinocytosis, as well as other nonmacropinocytic endocytosis pathways that are regulated by actin (52). Consequently, the efficiency of HIV-1 macropinocytosis and other actin-dependent endocytic processes involved in HIV uptake may be affected. However, the impact of spinoculation on the endocytotic activities in primary T cells remains to be determined.

Since the inhibition of internalization by EIPA is 30 to 50% in our experimental setting, the inhibition of macropinocytosis by EIPA might attenuate additional steps of the HIV-1 replication cycle in primary $CD4^+$ T cells. One possible mechanism by which EIPA inhibits HIV-1 infection is suppression of mTORC activity. mTORC activity correlates with efficient HIV-1 infection of primary $CD4^+$ T cells (43–46). However, AZD2014, a specific mTOR inhibitor that inhibits mTORC1 and mTORC2 activities, shows no or only a modest inhibitory effect on HIV-1 infection compared to EIPA in our experimental setting. Therefore, regardless of the involvement of mTORC, the primary effect of EIPA on HIV-1 infection is likely the inhibition of the cytoplasmic entry process of HIV-1, and this effect of EIPA is evident only in primary $CD4^+$ T cells but not in A3.01 cells.

HIV-1 uses macropinocytosis to enter primary $CD4^+$ T cells (shown by this study) and other cells (21–24). In addition to HIV-1, multiple virus species enter target cells via macropinocytosis (25–29). These observations suggest a possibility that macropinosomes provide beneficial environments for some viruses to enter target cells compared to the plasma membrane and other endosomal compartments. For example, proviral factors, e.g., viral receptors, may accumulate on macropinosome membranes. Macropinosomes contain HIV-1 coreceptor CCR5 and likely CXCR4 (53, 54). In addition, HIV-1 fusion within macropinosomes would require the presence of CD4 on the lumen surface of these structures, consistent with the observation that CD4 is present in forming macropinosomes (19). CD4, CCR5, and CXCR4 may be highly concentrated on the macropinosome membranes in primary $CD4^+$ T cells compared to the plasma membrane and/or other endosomal compartments. Inversely, it is also possible that antiviral factors, such as interferon-inducible transmembrane proteins, which localize to endosomes (55–57), may be excluded from macropinosomes. Specific membrane proteins are observed to be excluded from macropinosomes in *Dictyostelium* amoebae (58). This indicates the presence of a mechanism for the exclusion of specific proteins from macropinosomes during macropinocytosis. Whether proviral and antiviral host membrane proteins are enriched or excluded from macropinosomes remains to be determined.

In summary, we uncovered that macropinocytosis contributes to HIV-1 entry into primary $CD4^+$ T cells, which is not evident in T cell lines. Since macropinocytosis in primary $CD4^+$ T cells was only recently discovered, the molecular mechanisms are not well characterized. While the molecular mechanisms of macropinocytosis are similar across different cell types examined thus far, there are also significant differences (16–19). Fully understanding the molecular mechanism promoting macropinocytosis in primary $CD4^+$ T cells may identify a novel target for an antiretroviral strategy that specifically targets macropinocytosis in this cell type without adverse effects on other cell types.

Materials and Methods

Materials. Human peripheral blood mononuclear cells as well as human CD4+ T cell lines were cultured as detailed in *SI Appendix*. Construction of HIV-1 molecular clone plasmids (pNL4-3 and pCH040) that encode NanoLuc-IRES-nef (NI), SOS Env, or Gag-iNanoLuc is described in *SI Appendix* along with description of other plasmids used in the study.

Methods. Stocks of both engineered and nonengineered viruses were prepared via transfection of 293 T cells and used to test the effects of EIPA or J/B on steps in the infection process in NanoLuc-, microscopy-, and ELISA-based virus internalization assays, flow cytometry- and microscopy-based fusion assays, and NanoLuc-based infectivity assay. The extended methods used in these experiments and other control experiments are available in *SI Appendix*.

Data, Materials, and Software Availability. All study data are included in the article and/or *SI Appendix*. The raw visual data as well as the reagents used are available from A.O. upon request.

ACKNOWLEDGMENTS. We thank the members of the Ono laboratory for helpful discussions and critical reviews of the manuscript. We also thank Drs. Kathleen L. Collins and Andrew Mehle for the anti-HIV-1 p24 antibody (clone 31-90-25) and pBD-PASTN, respectively. The following reagents were obtained through the AIDS Research and Reference Reagent Program, Division of AIDS, National Institute of Allergy and Infectious Diseases, NIH: Panel of Full-Length Transmitted/Founder (T/F) HIV-1 Infectious Molecular Clones including CH040, pEGFP-Vpr, T-20, raltegravir, saquinavir, HIV-1 IIIB p24 recombinant protein, HIV-1 p24 monoclonal antibody (183-H12-5C), HIV-1 p24 monoclonal antibody (241-D), and TZM-bl cells from Drs. John C. Kappes, Warner C. Greene, Bruce Chesebro, Kathy Wehrly, Susan Zolla-Pazner, and Xiaoyun Wu, and Tranzyme Inc. We thank Drs. Warner C. Greene and Dorus Gadella for pCMV4-BlaM-Vpr and pmScarlet_C1, respectively. This work is supported by NIH Grants R01 AI165381 (to A.O. and P.D.K.).

Author affiliations: [a]Department of Microbiology & Immunology, University of Michigan Medical School, Ann Arbor, MI 48109; and [b]Microscopy core, Biomedical Research Core Facilities, Office of Research, University of Michigan Medical School, Ann Arbor, MI 48109

1. M. O. McClure, M. Marsh, R. A. Weiss, Human immunodeficiency virus infection of CD4-bearing cells occurs by a pH-independent mechanism. *EMBO J* **7**, 513–518 (1988).
2. B. S. Stein *et al.*, pH-independent HIV entry into CD4-positive T cells via virus envelope fusion to the plasma membrane. *Cell* **49**, 659–668 (1987).
3. P. J. Maddon *et al.*, HIV infection does not require endocytosis of its receptor, CD4. *Cell* **54**, 865–874 (1988).
4. A. Pelchen-Matthews, P. Clapham, M. Marsh, Role of CD4 endocytosis in human immunodeficiency virus infection. *J. Virol.* **69**, 8164–8168 (1995).

5. K. Miyauchi, Y. Kim, O. Latinovic, V. Morozov, G. B. Melikyan, HIV enters cells via endocytosis and dynamin-dependent fusion with endosomes. *Cell* **137**, 433–444 (2009).
6. J. Daecke, O. T. Fackler, M. T. Dittmar, H. G. Krausslich, Involvement of clathrin-mediated endocytosis in human immunodeficiency virus type 1 entry. *J. Virol.* **79**, 1581–1594 (2005).
7. L. von Kleist *et al.*, Role of the clathrin terminal domain in regulating coated pit dynamics revealed by small molecule inhibition. *Cell* **146**, 471–484 (2011).
8. M. Marin, Y. Kushnareva, C. S. Mason, S. K. Chanda, G. B. Melikyan, HIV-1 fusion with CD4+ T cells is promoted by proteins involved in endocytosis and intracellular membrane trafficking *Viruses* **11**, 100 (2019).
9. N. Herold, B. Muller, H. G. Krausslich, Reply to "Can HIV-1 entry sites be deduced by comparing bulk endocytosis to functional readouts for viral fusion?" *J. Virol.* **89**, 2986–2987 (2015).
10. M. Marin, G. B. Melikyan, Can HIV-1 entry sites be deduced by comparing bulk endocytosis to functional readouts for viral fusion? *J. Virol.* **89**, 2985 (2015).
11. T. Murakami, A. Ono, HIV-1 entry: Duels between Env and host antiviral transmembrane proteins on the surface of virus particles. *Curr. Opin. Virol.* **50**, 59–68 (2021).
12. M. Sharma, M. Marin, H. Wu, D. Prikryl, G. B. Melikyan, Human immunodeficiency virus 1 preferentially fuses with pH-neutral endocytic vesicles in cell lines and human primary CD4+ T-cells *ACS Nano.* **17**, 17436–17450 (2023).
13. M. de la Vega *et al.*, Inhibition of HIV-1 endocytosis allows lipid mixing at the plasma membrane, but not complete fusion. *Retrovirology* **8**, 99 (2011).
14. A. Aggarwal *et al.*, HIV infection is influenced by dynamin at 3 independent points in the viral life cycle. *Traffic* **18**, 392–410 (2017).
15. N. Herold *et al.*, HIV-1 entry in SupT1-R5, CEM-ss, and primary CD4+ T cells occurs at the plasma membrane and does not require endocytosis. *J. Virol.* **88**, 13956–13970 (2014).
16. G. J. Doherty, H. T. McMahon, Mechanisms of endocytosis. *Annu. Rev. Biochem.* **78**, 857–902 (2009).
17. J. C. Charpentier, P. D. King, Mechanisms and functions of endocytosis in T cells. *Cell Commun. Signal* **19**, 92 (2021).
18. J. A. Swanson, C. Watts, Macropinocytosis. *Trends Cell Biol.* **5**, 424–428 (1995).
19. J. C. Charpentier *et al.*, Macropinocytosis drives T cell growth by sustaining the activation of mTORC1. *Nat. Commun.* **11**, 180 (2020).
20. S. Yoshida, R. Pacitto, K. Inoki, J. Swanson, Macropinocytosis, mTORC1 and cellular growth control. *Cell Mol. Life Sci.* **75**, 1227–1239 (2018).
21. G. C. Carter, L. Bernstone, D. Baskaran, W. James, HIV-1 infects macrophages by exploiting an endocytic route dependent on dynamin, Rac1 and Pak1. *Virology* **409**, 234–250 (2011).
22. N. Q. Liu *et al.*, Human immunodeficiency virus type 1 enters brain microvascular endothelia by macropinocytosis dependent on lipid rafts and the mitogen-activated protein kinase signaling pathway. *J. Virol.* **76**, 6689–6700 (2002).
23. V. Marechal *et al.*, Human immunodeficiency virus type 1 entry into macrophages mediated by macropinocytosis. *J. Virol.* **75**, 11166–11177 (2001).
24. A. Yasen, R. Herrera, K. Rosbe, K. Lien, S. M. Tugizov, HIV internalization into oral and genital epithelial cells by endocytosis and macropinocytosis leads to viral sequestration in the vesicles. *Virology* **515**, 92–107 (2018).
25. J. Mercer, A. Helenius, Vaccinia virus uses macropinocytosis and apoptotic mimicry to enter host cells. *Science* **320**, 531–535 (2008).
26. E. de Vries *et al.*, Dissection of the influenza A virus endocytic routes reveals macropinocytosis as an alternative entry pathway. *PLoS Pathog.* **7**, e1001329 (2011).
27. J. Mercer, A. Helenius, Virus entry by macropinocytosis. *Nat. Cell Biol.* **11**, 510–520 (2009).
28. A. Nanbo *et al.*, Ebolavirus is internalized into host cells via macropinocytosis in a viral glycoprotein-dependent manner. *PLoS Pathog.* **6**, e1001121 (2010).
29. C. Shema Mugisha *et al.*, A simplified quantitative real-time PCR assay for monitoring SARS-CoV-2 growth in cell culture. *mSphere* **5**, e00658 (2020).
30. L. G. Abrahamyan, R. M. Markosyan, J. P. Moore, F. S. Cohen, G. B. Melikyan, Human immunodeficiency virus type 1 Env with an intersubunit disulfide bond engages coreceptors but requires bond reduction after engagement to induce fusion. *J. Virol.* **77**, 5829–5836 (2003).
31. J. M. Binley *et al.*, Redox-triggered infection by disulfide-shackled human immunodeficiency virus type 1 pseudovirions. *J. Virol.* **77**, 5678–5684 (2003).
32. J. M. Binley *et al.*, A recombinant human immunodeficiency virus type 1 envelope glycoprotein complex stabilized by an intermolecular disulfide bond between the gp120 and gp41 subunits is an antigenic mimic of the trimeric virion-associated structure. *J. Virol.* **74**, 627–643 (2000).
33. S. Veiga, S. Henriques, N. C. Santos, M. Castanho, Putative role of membranes in the HIV fusion inhibitor enfuvirtide mode of action at the molecular level. *Biochem J* **377**, 107–110 (2004).
34. G. B. Melikyan *et al.*, Evidence that the transition of HIV-1 gp41 into a six-helix bundle, not the bundle configuration, induces membrane fusion. *J. Cell Biol.* **151**, 413–423 (2000).
35. M. Koivusalo *et al.*, Amiloride inhibits macropinocytosis by lowering submembranous pH and preventing Rac1 and Cdc42 signaling. *J. Cell Biol.* **188**, 547–563 (2010).
36. M. Cavrois, C. De Noronha, W. C. Greene, A sensitive and specific enzyme-based assay detecting HIV-1 virion fusion in primary T lymphocytes. *Nat. Biotechnol.* **20**, 1151–1154 (2002).
37. T. Sakai *et al.*, Dual wavelength imaging allows analysis of membrane fusion of influenza virus inside cells. *J. Virol.* **80**, 2013–2018 (2006).
38. S. B. Kutluay *et al.*, Global changes in the RNA binding specificity of HIV-1 Gag regulate virion genesis. *Cell* **159**, 1096–1109 (2014).
39. Q. Li *et al.*, Encapsulating quantum dots within HIV-1 Virions through site-specific decoration of the matrix protein enables single virus tracking in live primary macrophages. *Nano. Lett.* **18**, 7457–7468 (2018).
40. E. Besnard *et al.*, The mTOR complex controls HIV latency. *Cell Host Microbe* **20**, 785–797 (2016).
41. J. M. Crater, D. F. Nixon, R. L. Furler O'Brien, HIV-1 replication and latency are balanced by mTOR-driven cell metabolism. *Front Cell Infect. Microbiol.* **12**, 1068436 (2022).
42. S. Jin *et al.*, TSC1 and DEPDC5 regulate HIV-1 latency through the mTOR signaling pathway. *Emerg. Microbes. Infect.* **7**, 138 (2018).
43. H. E. Taylor *et al.*, mTOR overcomes multiple metabolic restrictions to enable HIV-1 reverse transcription and intracellular transport. *Cell Rep.* **31**, 107810 (2020).
44. A. Heredia *et al.*, Targeting of mTOR catalytic site inhibits multiple steps of the HIV-1 lifecycle and suppresses HIV-1 viremia in humanized mice. *Proc. Natl. Acad. Sci. U. S. A.* **112**, 9412–9417 (2015).
45. D. Planas *et al.*, HIV-1 selectively targets gut-homing CCR6+CD4+ T cells via mTOR-dependent mechanisms. *JCI Insight* **2**, e93230 (2017).
46. G. Singh *et al.*, HIV-1 hypermethylated guanosine cap licenses specialized translation unaffected by mTOR. *Proc. Natl. Acad. Sci. U. S. A.* **119**, e2105153118 (2022).
47. E. L. Racoosin, J. A. Swanson, Macropinosome maturation and fusion with tubular lysosomes in macrophages. *J. Cell Biol.* **121**, 1011–1020 (1993).
48. S. Yoshida, R. Pacitto, Y. Yao, K. Inoki, J. A. Swanson, Growth factor signaling to mTORC1 by amino acid-laden macropinosomes. *J. Cell Biol.* **211**, 159–172 (2015).
49. L. J. Hewlett, A. R. Prescott, C. Watts, The coated pit and macropinocytic pathways serve distinct endosome populations. *J. Cell Biol.* **124**, 689–703 (1994).
50. D. Eggink *et al.*, HIV-1 anchor inhibitors and membrane fusion inhibitors target distinct but overlapping steps in virus entry. *J. Biol. Chem.* **294**, 5736–5746 (2019).
51. J. Guo, W. Wang, D. Yu, Y. Wu, Spinoculation triggers dynamic actin and cofilin activity that facilitates HIV-1 infection of transformed and resting CD4 T cells. *J. Virol.* **85**, 9824–9833 (2011).
52. A. S. Robertson, E. Smythe, K. R. Ayscough, Functions of actin in endocytosis. *Cell. Mol. Life Sci.* **66**, 2049–2065 (2009).
53. E. B. Cepeda *et al.*, Mechanisms regulating cell membrane localization of the chemokine receptor CXCR4 in human hepatocarcinoma cells. *Biochim. Biophys. Acta* **1853**, 1205–1218 (2015).
54. Z. Liu, E. Xu, H. T. Zhao, T. Cole, A. B. West, LRRK2 and Rab10 coordinate macropinocytosis to mediate immunological responses in phagocytes. *EMBO J* **39**, e104862 (2020).
55. G. Shi, O. Schwartz, A. A. Compton, More than meets the I: The diverse antiviral and cellular functions of interferon-induced transmembrane proteins. *Retrovirology* **14**, 53 (2017).
56. S. Majdoul, A. A. Compton, Lessons in self-defence: Inhibition of virus entry by intrinsic immunity. *Nat. Rev. Immunol.* **22**, 339–352 (2022).
57. G. M. Jakobsdottir *et al.*, On the whereabouts of HIV-1 cellular entry and its fusion ports. *Trends Mol. Med.* **23**, 932–944 (2017).
58. K. Ravanel *et al.*, Membrane sorting in the endocytic and phagocytic pathway of Dictyostelium discoideum. *Eur. J. Cell Biol.* **80**, 754–764 (2001).